ELSEVIER

Journal of Organometallic Chemistry 565 (1998) 217–224

Journal of Organometallic Chemistry

Five-coordinate hydrogen in hydrido rhodium cluster compounds: A theoretical analysis[1]

Régis Gautier, Jean-François Halet *

Laboratoire de Chimie du Solide et Inorganique Moléculaire, UMR CNRS 6511 Université de Rennes 1, Avenue du Général Leclerc, 35042 Rennes-Cedex, France

Received 17 December 1997

Abstract

The electronic structure of the hydrido species $[H_2Rh_{13}(CO)_{24}]^{3-}$ containing H atoms inserted in square pyramidal holes is analyzed using DFT calculations. In particular, the covalent nature of the hydrogen-metal bonding is demonstrated, due to an effective interaction of the H orbitals with high-lying FMOs of the centered anti-cuboctahedral Rh_{13} core. The position of the hydrogen atoms in the square pyramidal cavities is mainly governed by the arrangement of the carbonyl ligands tethered to the metallic square faces. In agreement with the structural data, DFT computations favors the isomer with the H atoms encapsulated in the cavities having the smallest number of bridging CO ligands. © 1998 Elsevier Science S.A. All rights reserved.

Keywords: Hydrido; Density functional calculations; Five co-ordinate hydrido; Interstitial hydrido clusters

1. Introduction

Hydrido carbonyl cluster compounds represent interesting molecular models for the coadsorption of hydrogen and carbon monoxide on metal surfaces or the storage of hydrogen in metals [1]. In these species the hydrogen atoms either enter a cavity as in $[Ru_6(CO)_{18}(\mu_6\text{-H})]^-$ [2], or are surface located as in $[Os_{10}(CO)_{24}(\mu_3\text{-H})_2(\mu\text{-H})_2]^{2-}$ [1,3]. Among the compounds containing fully encapsulated hydrogen atoms, the anions $[H_nRh_{13}(CO)_{24}]^{(5-n)-}$ $(n = 1–4)$ provide a unique series of isostructural, multihydride clusters [4–9]. Different studies indicate that they are interconvertible by addition or removal of one or more protons. Surprisingly enough, the penta-anionic cluster $[Rh_{13}(CO)_{24}]^{5-}$ and the neutral cluster $H_5Rh_{13}(CO)_{24}$ have not yet been observed. Furthermore, kinetic and thermodynamic studies indicate that the monohydride species $[HRh_{13}(CO)_{24}]^{4-}$ is less stable than the di- and tri-hydride adducts in acetonitrile for instance [8]. This indicates that few interstitial hydrogen atoms stabilize such a structural arrangement, but too many seem to be unpropitious.

The mono-, di-, and tri-hydride derivatives have all been isolated as crystalline solids and examined by X-ray crystallography [4,6,7]. They have similar structural arrangements consisting of a centered anti-cuboctahedron i.e. a hexagonal close-packed metal skeleton in which each surface rhodium atom is coordinated to one terminal and two bridging carbonyls. The hydride ligands were not directly located in the X-ray studies but were suggested to be close to the square faces of the square pyramidal metallic cavities, in agreement with NMR data [9]. This was confirmed recently by a neutron diffraction analysis of the hydrido cluster complex $[H_2Rh_{13}(CO)_{24}]^{3-}$ (**1**) performed by Bau et al. at low temperature [10,11]. The two hydrogen atoms are located in two of the six square pyramidal holes (**2a**), in positions almost coplanar with the four basal (surface)

* Corresponding author. Fax: +33 2 99635704; e-mail: halet@univ-rennes1.fr

[1] Dedicated to Professor Michael Bruce on the occasion of his 60th birthday.

PII S0022-328X(98)00457-4

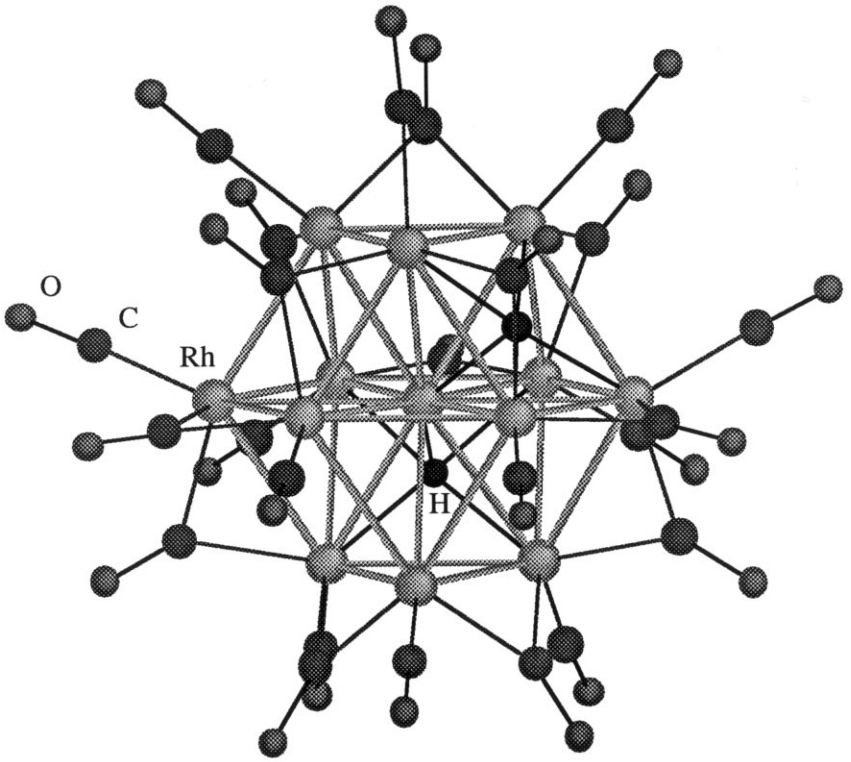

1

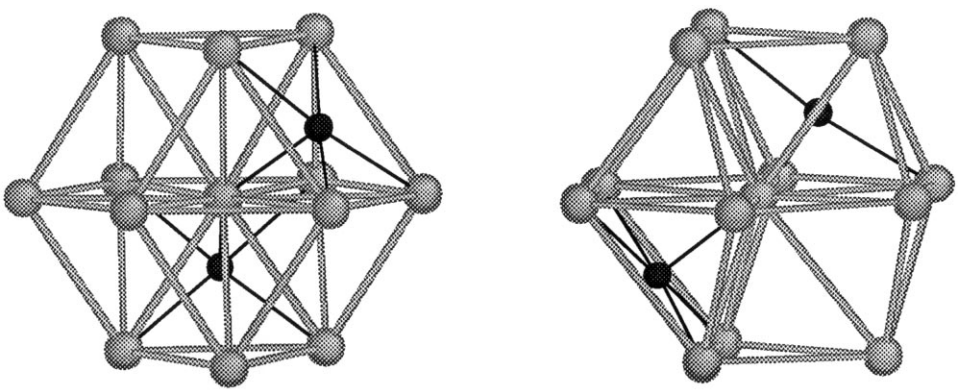

a **b**

2

Rh atoms of each square pyramidal cavity, slightly displaced toward the central atom of the cluster core (**2b**). In both cases, the axial Rh(central)–H distance is shorter (average 1.84 Å) than the four Rh(surface)–H distances (average, 1.97 Å).

We may ask why the H atoms are not disordered at low temperature over the six available square pyramidal sites. Indeed, the D_{3h} symmetry group of the cluster is reduced to C_s due to the particular arrangement of the CO ligands, creating only four inequivalent types of square pyramidal holes before incorporation of the H atoms (denoted a–d, see **3**). Nevertheless, only two positions out of four are occupied in **1**. The size of the occupied sites is slightly larger than the empty sites (average, 0.03 Å), but this weak size difference is not sufficient by itself to fully explain the observed ordering

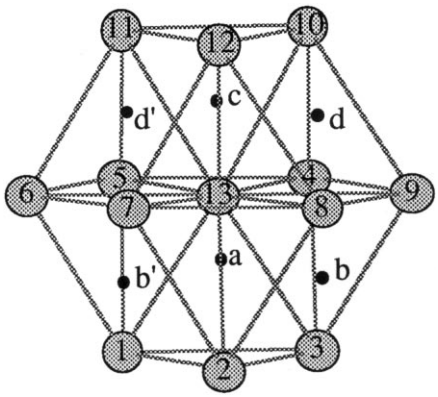

3

of the hydrogen atoms in species **1**.

The structural characterization of cluster **1** containing unusual five-coordinate hydrogen atoms prompted us to analyze its electronic structure and the bonding of the inserted H atoms with their metallic host. To this purpose, theoretical calculations using the extended Hückel (EH) and density-functional theory (DFT) methods were carried out [12–17].

2. Theoretical considerations

As expected from the extension of the Polyhedral Skeletal Electron Pair (PSEP) theory to high-nuclearity metal carbonyl clusters [18], the compounds $[H_nRh_{13}(CO)_{24}]^{(5-n)-}$ ($n = 1$–4) have 170 cluster valence electrons (CVE) (9(Rh) × 13 + 2(CO) × 24 + 1(H or negative charge) × 5). Indeed, these compounds are four-connected polyhedral molecules, generally characterized by a total of $14n + 2l$ CVEs [19].

DFT calculations were first carried out on the hypothetical model $[Rh_{13}(CO)_{24}]^{5-}$ of C_s symmetry (the Rh–CO geometry of **1** was taken), in order to understand the electronic properties of the metallic host [14–17]. Although, such an anion has not yet been observed experimentally, a rather large HOMO/LUMO gap between bonding and non-bonding, and antibonding orbitals is computed for the count of 170 CVEs, as illustrated in Fig. 1. The DFT-MO picture of $[Rh_{13}(CO)_{24}]^{5-}$ supports previous EH results obtained by Mingos and Lin on the centered anti-cuboctahedral model $Rh_{13}H_{36}$ [20]. According to these authors, such molecules are associated with a total of 13 skeletal bonding molecular orbitals (MO) which lie in a rather narrow energy range. Four of them are σ-type MOs ($a_1' + e' + a_2''$ in D_{3h} symmetry) and 9 are π-type MOs ($2a_1' + 2e' + e'' + a_2''$ in D_{3h} symmetry) [20]. When occupied, these skeletal MOs are responsible for the cohesion of the cluster core. The lowering of symmetry in our model leads to important orbital mixing, rendering difficult the identification of the skeletal MOs accounting for the metal–metal bonding. Nevertheless, some of the MOs in the HOMO region can be recognized as skeletal orbitals. For instance, MOs 128a′ (the HOMO for the count of 170 CVEs), 105a″, and 127a′ can be identified as being the corresponding π-type MOs of a_1' and e symmetry in the $Rh_{13}H_{36}$ model. The 126a′ MO corresponds to the totally symmetrical σ-type a_1' MO resulting from the interaction of the s orbital of the central rhodium atom with surface-metal MOs of the same symmetry. The 104a″ MO is one of the π-type skeletal MOs. Other skeletal MOs are contained in sets of MOs lower in energy.

The antibonding block of MOs positioned above the HOMO, derives mainly from the out-of-phase combinations of the d orbitals of the interstitial rhodium atom and outer-sphere MO of the Rh_{12} cage [20].

DFT calculations were then performed on $[H_2Rh_{13}(CO)_{24}]^{3-}$ with H atoms located in their experimental positions (H^a and H^d in **3**). The symmetry of the molecule is lowered to C_1, allowing important mixing. However, it is remarkable that mainly three frontier molecular orbitals (FMO) of the $Rh_{13}(CO)_{24}$ fragment dominate the interaction with the hydrogen orbitals. The π-type 128a′ MO interacts strongly with the out-of-phase $(H)_2$ orbitals. To a lesser extent, the 105a″ interacts with both the in-phase and out-of-phase hydrogen combinations. The main bonding interaction occurs between the σ-type 126a′ metallic MO and the in-phase combination of hydrogen orbitals. The result of these interactions is the opening of the HOMO/LUMO gap from 0.67 eV for the $[Rh_{13}(CO)_{24}]^{5-}$ anion to 0.88 eV for the hydrogen $[H_2Rh_{13}(CO)_{24}]^{3-}$ species (see Fig. 1). Interestingly enough, some hydrogen participation is noted in the MOs situated in the HOMO region up to 5% as in the 231a MO.

From these results, we conclude that these metallic FMOs must govern the ordering of the H atoms at low temperature in $[H_2Rh_{13}(CO)_{24}]^{3-}$. This can be partially inferred from a glance at the plots of some FMOs of $[Rh_{13}(CO)_{24}]^{5-}$. For instance, as it is clearly shown in Fig. 2, the 128a′ MO (HOMO for the $[Rh_{13}(CO)_{24}]^{5-}$ ion) is importantly localized on the central rhodium atom Rh (13) extending largely towards sites a and d, but very poorly towards sites c and b. Contour plots in square planes of the Rh_{13} core indicate also some metallic localization around sites a and d. Consequently, this MO is suitable for a strong interaction with orbitals of hydrogen atoms located in sites a and d rather than in sites b and c. Extension of the 105a″ MO is appropriate for interacting with orbitals of H atoms sitting in positions b and d (see Fig. 3). The 127a′ and 104a″ MOs have their larger amplitude away from the different hydrogen sites, and are thus not suitable for effective interaction with the inserted H atoms (see

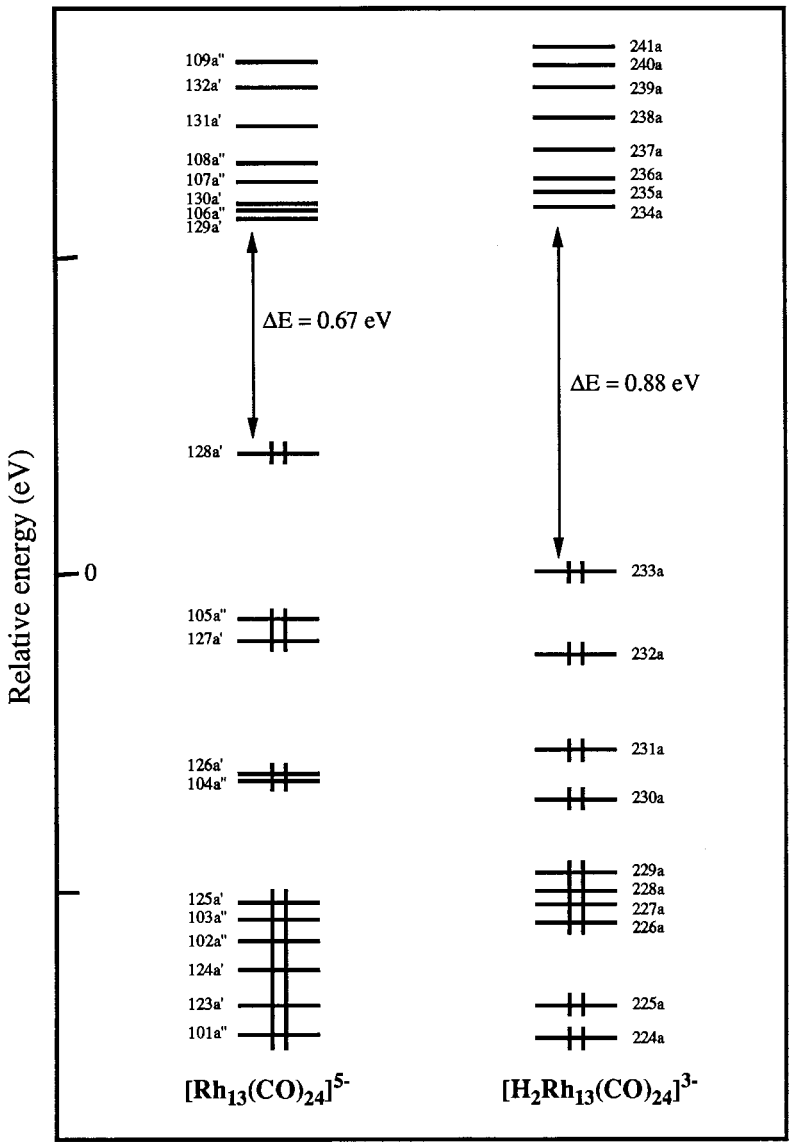

Fig. 1. DFT energy level diagram for the $[Rh_{13}CO)_{24}]^{5-}$ and $[H_2Rh_{13}CO)_{24}]^{3-}$ anions.

Figs. 4 and 5, respectively). On the other hand, the 126a′ MO displays lobes directed toward sites a and d as illustrated in Fig. 6, particularly localized on the central rhodium atom, allowing some interaction with orbitals of H atoms in these sites (Figs. 2–6).

These considerations indicate that hydrogen atoms should prefer to occupy sites a and d rather than sites b and c in $[H_2Rh_{13}(CO)_{24}]^{3-}$, as experimentally observed (vide supra). Among factors which may determine the preferred sites for the inserted H atoms in species **1**, there are the distance between the two hydrogen atoms and the arrangement of the CO ligands attached to the metallic square faces. Assuming a regular Rh_{13} cage, the shortest distances between 'holes' is ca. 2.25 Å (between sites a and c and sites b and d), whereas the largest distance is ca. 3.55 Å (between sites a and d for instance). Intermediate separations of ca. 2.75 Å are measured between other sites such as a and b. Different CO environments are experimentally observed for the six square pyramidal cavities. Four terminal CO and one bridging CO ligands surround site a. Site b is located in a cavity having four terminal CO and three bridging CO ligands. Cavity c is the only one that has four bridging CO in addition to four terminal CO groups. Finally, site d is surrounded by four terminal and two bridging COs [10].

Qualitative EH calculations were performed on a modelized $[H_2Rh_{13}(CO)_{24}]^{3-}$ varying the positions of the two H atoms. Assuming a $Rh_{13}(CO)_{24}$ core of C_s symmetry, nine different isomeric forms are possible. In agreement with experiments, the isomer with H atoms in sites a and d is preferred, between roughly 0.15 to 0.5 eV, over the other isomers. This is supported by DFT computations. For instance, the isomer with H atoms in

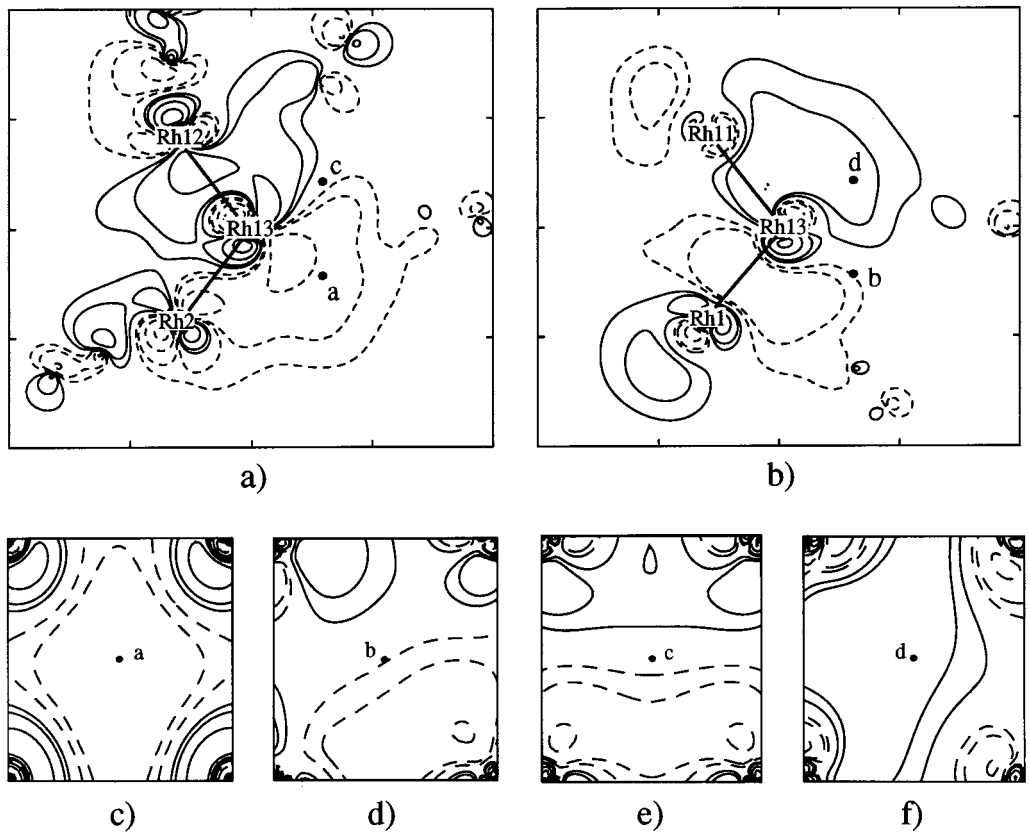

Fig. 2. Contour plots of the 128a′ MO of $[Rh_{13}CO)_{24}]^{5-}$: (a) in plane Rh(2)–Rh(13)–Rh(12); (b) in plane Rh(1)–Rh(13)–Rh(11); c) in plane Rh(1)–Rh(3)–Rh(4)–Rh(5); (d) in plane Rh(2)–Rh(3)–Rh(8)–Rh(9); (e) in plane Rh(4)–Rh(5)–Rh(10)–Rh(11); (f) in plane Rh(8)–Rh(9)–Rh(10)–Rh(12). Contour values are ± 0.01, ± 0.02, ± 0.05, ± 0.10, ± 0.20, ± 0.50 (e bohr$^{-3})^{1/2}$.

sites a and b is 0.24 eV less stable than that with H atoms inserted in positions a and d. The energetic distribution of the different isomers seems to indicate that the location of the H atoms in species **1** might depend primarily on the CO environment of the square faces rather than the H···H separations. Encapsulated H atoms tend to occupy sites having the minimum number of bridging COs. As said above, cavities a and d have only one and two bridging COs, respectively. Metallic orbitals being less involved in M-(μ-CO) bonding are more effective to interact with the inserted H atoms. This statement is supported by EH calculations performed on the monohydride $[HRh_{13}(CO)_{24}]^{4-}$ species, which show that the incorporated H atom is preferentially located in site a.

Large elements incorporated in square pyramidal cavities such as carbon or nitrogen are usually exposed slightly below the center of the metallic basal plane away from the apical metal center, as illustrated in $Fe_5(CO)_{15}(\mu_5$-C) for instance [21]. Theoretical works indicate that this displacement is sensitive to the charge on the exposed atom [22]. It moves away from the square face as its negative charge increases. Contrarily to carbon or nitrogen, H atoms in species **1** are slightly displaced from the middle of the square faces but in an inward fashion, toward the apical rhodium atom of the cavities [10]. We think that this is mainly due not only to the size but also to the charge of the inserted H atoms. Indeed, using the analysis of Hirschfeld [23] obtained within DFT calculations, the encapsulated H atoms are nearly neutral (with charges of -0.10 and -0.09 for H^a and H^d, respectively).

3. Conclusion

The theoretical study of the hydrido species $[H_2Rh_{13}(CO)_{24}]^{3-}$ containing H atoms inserted in square pyramidal holes has allowed the understanding of the bonding mode of the H atoms with their metallic host. In particular, the covalent nature of the hydrogen–metal bonding has been demonstrated, due to an effective interaction of the H orbitals with high-lying FMOs of the centered anti-cuboctahedral Rh_{13} core. The position of the hydrogen atoms in the square pyramidal cavities is mainly governed by the arrangement of the carbonyl ligands tethered to the metallic square faces. In agreement with the structural data, DFT computations favor the isomer with the H atoms in sites a and d, that is in the cavities having the

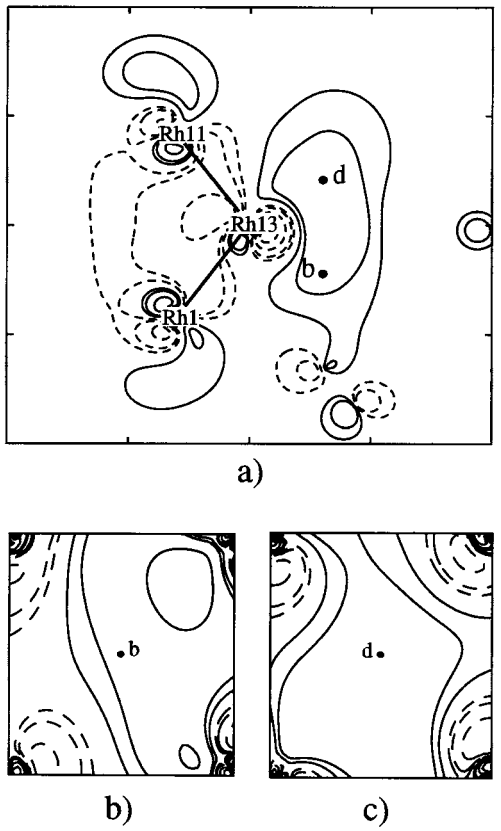

smallest number of bridging CO ligands. The results discussed here give some confidence in the use of DFT calculations in the location of hydrogen ligands in high nuclearity transition metal carbonyl clusters when direct location is not possible experimentally.

^{1}H-NMR measurements show that the interstitial H atoms are mobile at r.t. [10]. Although the energy difference between isomers is significant at low temperature in favor of that with H atoms located in sites a and d, it is sufficiently small to explain why hydrogen atoms are delocalized over different sites when the temperature increases. The obvious route to go from one square pyramidal hole to another is a path through inner triangular faces and tetrahedral cavities of the cluster.

One major question, not addressed here, remains. The parameters which determine whether or not a hydrogen atom enters a square pyramidal hole are not yet fully understood. Hydrogen atoms are fully encapsulated in holes in species **1**, whereas they are edge-bridging in the capped square pyramidal cluster

Fig. 3. Contour plots of the 105a″ MO of $[Rh_{13}CO)_{24}]^{5-}$: a) in plane Rh(1)–Rh(13)–Rh(11); b) in plane Rh(2)–Rh(3)–Rh(8)–Rh(9); c) in plane Rh(8)–Rh(9)–Rh(10)–Rh(12). See caption to Fig. 2 for contour values.

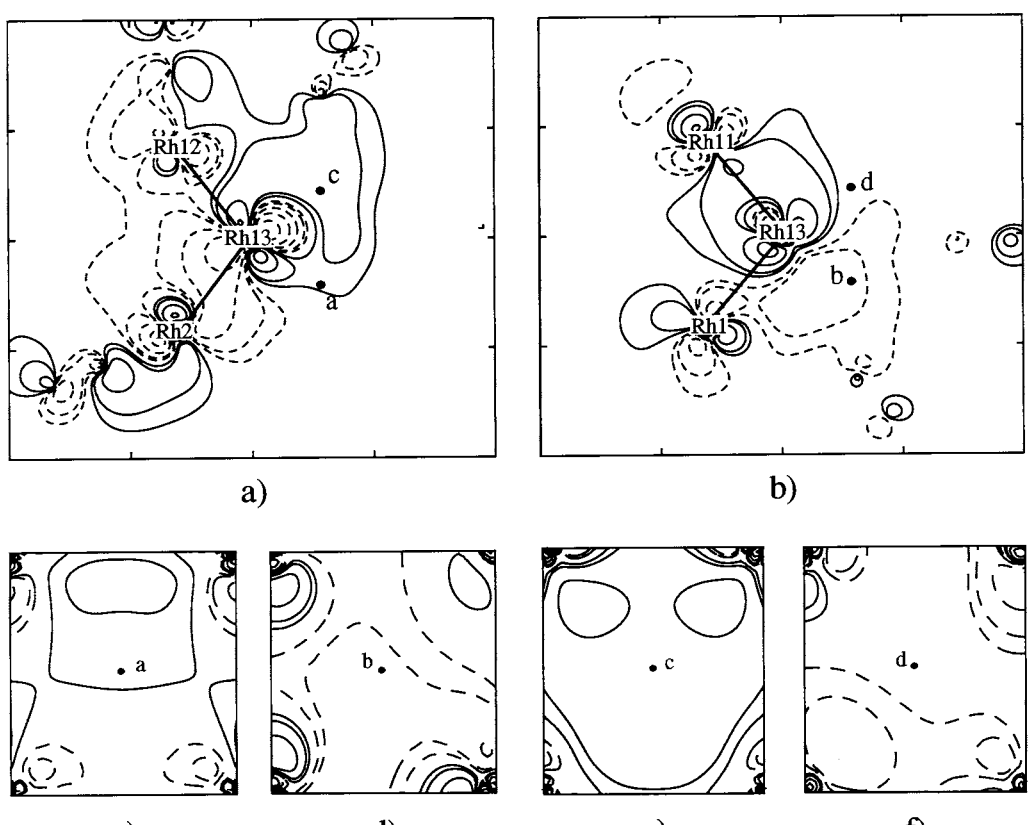

Fig. 4. Contour plots of the 127a′ MO of $[Rh_{13}CO)_{24}]^{5-}$: a) in plane Rh(2)–Rh(13)–Rh(12); b) in plane Rh(1)–Rh(13)–Rh(11); c) in plane Rh(1)–Rh(3)–Rh(4)–Rh(5); d) in plane Rh(2)–Rh(3)–Rh(8)–Rh(9); e) in plane Rh(4)–Rh(5)–Rh(10)–Rh(11); f) in plane Rh(8)–Rh(9)–Rh(10)–Rh(12). See caption to Fig. 2 for contour values.

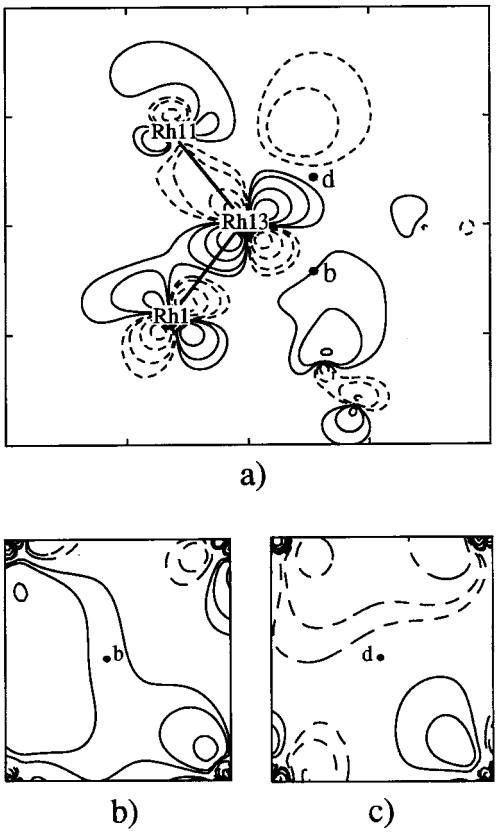

Fig. 5. Contour plots of the 104a″ MO of $[Rh_{13}CO)_{24}]^{5-}$: a) in plane Rh(1)–Rh(13)–Rh(11); b) in plane Rh(2)–Rh(3)–Rh(8)–Rh(9); c) in plane Rh(8)–Rh(9)–Rh(10)–Rh(12). See caption to Fig. 2 for contour values.

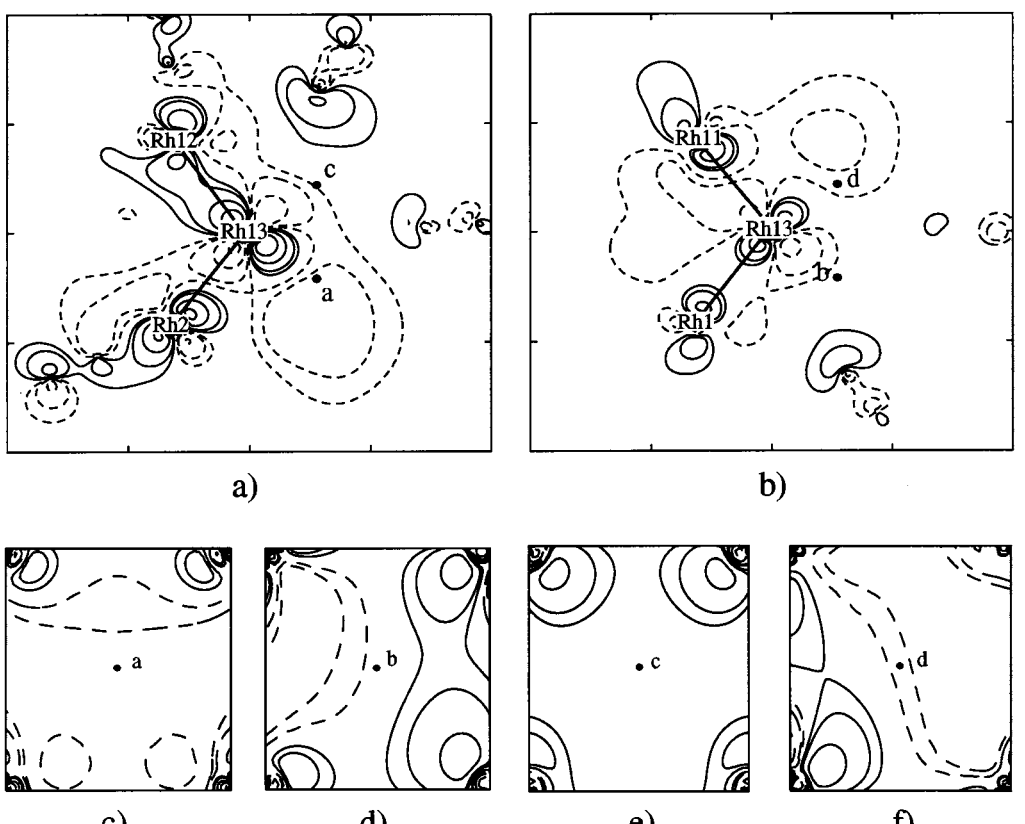

Fig. 6. Contour plots of the 126a′ MO of $[Rh_{13}CO)_{24}]^{5-}$: a) in plane Rh(2)–Rh(13)–Rh(12); b) in plane Rh(1)–Rh(13)–Rh(11); c) in plane Rh(1)–Rh(3)–Rh(4)–Rh(5); d) in plane Rh(2)–Rh(3)–Rh(8)–Rh(9); e) in plane Rh(4)–Rh(5)–Rh(10)–Rh(11); f) in plane Rh(8)–Rh(9)–Rh(10)–Rh(12). See caption to Fig. 2 for contour values.

$H_2Os_6(CO)_{18}$ for instance [11,24]. DFT calculations on different hydrido cluster species are in progress in order to fully appreciate the bonding of hydrogen atoms in such compounds.

Acknowledgements

Thanks are expressed to Professor R. Bau (University of Southern California, Los Angeles) for provision of some structural data and Professor J.-Y. Saillard (Université de Rennes 1, Rennes)) for helpful comments. Professor Baerends and Dr te Velde (Vrije Universiteit, Amsterdam) are acknowledged for introducing the authors to the ADF program. Exchanges between the groups of Amsterdam and Rennes have been made possible through an European Human Capital and Mobility Network (ERBCHRXCT-930156). J.-F. H. thanks the Centre de Ressources Informatiques (CRI) of Rennes and the Institut de Développement et de Ressources en Informatique Scientifique (IDRIS-

CNRS) of Orsay (project 970649) for computing facilities.

References

[1] L.H. Gade, B.F.G. Johnson, J. Lewis, Croat. Chem. Acta 68 (1995) and references therein.

[2] C.R. Eady, B.F.G. Johnson, J. Lewis, M.C. Malatesta, P. Machin, M. McPartlin, J. Chem. Soc. Chem. Commun. (1976) 945.

[3] A. Bashall, L.H. Gade, J. Lewis, B.F.G. Johnson, G.J. McIntyre, M. McPartlin, Angew. Chem. Int. Ed. Engl. 30 (1991) 1164.

[4] V.G. Albano, A. Ceriotti, P. Chini, G. Ciani, S. Martinengo, W.M. Anker, J. Chem. Soc. Chem. Commun. (1975) 859.

[5] S. Martinengo, B.T. Heaton, R.J. Goodfellow, P. Chini, J. Chem. Soc. Chem. Commun. (1977) 39.

[6] V.G. Albano, G. Ciamician, G. Ciani, S. Martinengo, A. Sironi, J. Chem. Soc. Dalton Trans. (1979) 978.

[7] G. Ciani, A. Sironi, S. Martinengo, J. Chem. Soc. Chem. Commun. (1981) 519.

[8] R.T. Weberg, J.R. Norton, J. Am. Chem. Soc. 112 (1990) 1105.

[9] C. Allevi, B.T. Heaton, C. Seregni, L. Strona, R.J. Goodfellow, P. Chini, S. Martinengo, J. Chem. Soc. Dalton Trans. (1986) 1375.

[10] R. Bau, M.H. Drabnis, L. Garlaschelli, W.T. Klooster, Z. Xie, T.F. Koetzle, S. Martinengo, Science 275 (1997) 1099.

[11] R. Bau, M.H. Drabnis, Inorg. Chim. Acta 259 (1997) 27.

[12] Extended Hückel calculations were carried out on the species $[H_2Rh_{13}(CO)_{24}]^{3-}$ varying the positions of the hydrogen atoms. The Rh_{13} core was somewhat idealized with the size of the six square pyramidal cavities equal. The program CACAO was used for the calculations [13]. The exponents ζ) and the valence shell ionization potentials H_{ii} in eV) were respectively): 1.3, −13.6 for H 1s; 1.625, −21.4 for C 2s; 1.625, −11.4 for C 2p; 2.275, −32.3 for O 2s; 2.275, −14.8 for O 2p; 2.135, −9.19 for Rh 5s; 2.100, −4.47 for Rh 5p. H_{ii} value for Rh 4d was set equal to −13.58. A linear combination of two Slater-type orbitals of exponents $\zeta_1 = 4.29$ and $\zeta_2 = 1.97$ with the weighting coefficients $c_1 = 0.5807$ and $c_2 = 0.5685$ was used to represent the Rh 4d atomic orbitals.

[13] C. Mealli, D. Proserpio, J. Chem. Educ. 67 (1990) 399.

[14] Density functional theory calculations were carried out on different Rh_{13} clusters using the Amsterdam Density Functional ADF) program [15] developed by Baerends and coworkers [16]. Electron correlation was treated within the local density approximation [17]. The atom electronic configurations were described by a triple-ζ STO basis set for Rh 4s, 4p, 4d, and 5s, augmented with a single-ζ 5p polarization function, a triple-ζ STO basis set for C and O, 2s and 2p, augmented with a single-ζ 3d polarization function, and a triple-ζ STO basis set for H 1s, augmented with a single-ζ 2p polarization function. A frozen-core approximation was used to treat the core electrons of Rh, C, and O. The experimental $Rh_{13}CO)_{24}$ fragment was taken for all calculations.

[15] Amsterdam Density Functional (ADF) program, release 2.3, Vrije Universteit, Amsterdam, The Netherlands, 1997.

[16] a) E.J. Baerends, D.E. Ellis, P. Ros, Chem. Phys. 2 (1973) 41. b) E.J. Baerends, P. Ros, Int. J. Quantum Chem. S12 (1978) 169. c) P.M. Boerrigter, G. te Velde, E.J. Baerends, Int. J. Quantum Chem. 33 (1998) 87. d) G. te Velde, E.J. Baerends, J. Comp. Phys. 99 (1992) 84.

[17] S.D. Vosko, L. Wilk, M. Nusair, Can. J. Chem. 58 (1990) 1200.

[18] D.M.P. Mingos, J. Chem. Soc. Chem. Commun. (1985) 1352.

[19] a) R.L. Johnston, D.M.P. Mingos, J. Organomet. Chem. 280 (1985) 419. b) R.L. Johnston, D.M.P. Mingos, Struc. Bond. Berlin) 68 (1987) 29.

[20] a) D.M.P. Mingos, L. Zhenyang, J. Organomet. Chem. 341 (1988) 523. b) D.M.P. Mingos, L. Zhenyang, J. Chem. Soc. Dalton Trans. (1988) 1657.

[21] E.H. Braye, L.F. Dahl, W. Hübel, D.L. Wampler, J. Am. Chem. Soc. 84 (1962) 4633.

[22] a) J.-F. Halet, J.-Y. Saillard, R. Lissillour, M.J. McGlinchey, G. Jaouen, Organometallics 5 (1986) 139. b) J.-F. Halet, in: M. Gielen (Ed.) Topics in Physical Organometallic Chemistry, vol. 4, Freund Publishing House, London, 1992, p. 221, and references therein.

[23] F.L. Hirschfeld, Theor. Chim. Acta 44 (1977) 129.

[24] a) A.G. Orpen, J. Chem. Soc. Dalton Trans. (1980) 2509. b) R. Bau, S.A. Mason, L. Li, W.-T. Wong, J. Am. Chem. Soc. 119 (1997) 11992.